

phys. stat. sol. (b) **122**, 591 (1984)

Subject classification: 13.1; 1.3; 21.1; 21.2

*Institute of Materials Science,  
Academy of Mining and Metallurgy, Cracow<sup>1)</sup>*

## Electronic Processes in Electrode Materials of $A_xMX_2$ -Type <sup>2)</sup>

By

JANINA MOLEND

Electronic processes taking place during intercalation in  $A_xMX_2$ -type electrode materials ( $A = \text{Li, Na}$ ;  $M = \text{transition metal}$ ;  $X = \text{O, S}$ ) are discussed. It is shown that for cobalt bronze,  $\text{Na}_x\text{CoO}_{2-y}$ , taken as representative of the electrode materials under consideration, the variation of Co-Co interactions, accompanying the intercalation process, leads to the modification of band structure of the cathode material bringing about the Mott transition of metal-non-metal type. The experimental results indicate close correlation between the electronic structure of the cathode material and its potential.

Dans ce travail on a considéré les processus électroniques dans les matériaux d'électrode de type  $A_xMX_2$  ( $A = \text{Li, Na}$ ;  $M = \text{métal de transition}$ ;  $X = \text{O, S}$ ). Sur la base du bronze de cobalt  $\text{Na}_x\text{CoO}_{2-y}$  on a montré, que les changements des interactions Co-Co pendant l'intercalation électrochimique conduit à la modification de la structure de bande du matériau de cathode en provoquant la transition de Mott de type métal-non-métal. Les résultats des études mettent en évidence la corrélation entre la structure électronique du matériau de cathode et son potentiel.

### 1. Introduction

Recently extensive studies [1 to 3] have been carried out on nonstoichiometric compounds, which can reversibly incorporate foreign atoms in their lattice without any important modification of local configuration of atoms or crystallographic structure. A wide group of compounds capable of intercalating alkaline metals is that of transition metal dichalcogenides of  $MX_2$ -type ( $M$  transition metal;  $X = \text{O, S}$ ). The said compounds are characteristic layered structures. Alkaline atoms take the positions between the layers. Weak interactions of van der Waals type between the  $(MX_2)_n$  layers favour the intercalation reaction already at room temperature.

The  $A_xMX_2$  compounds ( $A$  alkaline metal) exhibit a mixed, ionic-electronic conductivity. The ionic conductivity is related to the presence of mobile alkaline ions. The electronic conductivity is by several orders of magnitude higher and exhibits as a rule metallic character, typical of the majority of compounds with layered structure. The structural and transport properties of those compounds enable their possible application as electrode materials in alkaline cells.

In the present paper, the electronic structure of the cathode material has been related to the character of the electrode potential variations with the concentration of intercalated species and an electronic model of the intercalation process has been proposed. In order to confirm the said model, the experimental results obtained with

<sup>1)</sup> Al. Mickiewicza 30, 30059 Cracow, Poland.

<sup>2)</sup> A part of experimental work has been carried out in Laboratoire de Chimie du Solide du C.N.R.S., Université de Bordeaux I, France.

$\text{Na}_x\text{CoO}_{2-y}$  cobalt bronze have been used. Furthermore, to simplify the model, a P2-type bronze has been selected for this study, as it does not undergo any structural transitions.

The properties of the cobalt bronze  $\text{Na}_x\text{CoO}_{2-y}$  have been presented earlier [4, 5].

## 2. Theory

During the electrochemical intercalation



an alkaline ion is introduced into the structure of the cathode material. It takes the position between the layers built up of the  $(\text{MX}_6)$  octahedra in which the central position is occupied by a transition metal. The intercalation of an  $A^+$  ion in the cathode material is accompanied by transport of one electron from the anode to the cathode through the outer circuit.

In the  $\text{A}_x\text{MX}_2$ -type compounds [6] the band structure is formed mainly from the 3d-orbitals of the transition metal. The intercalated alkaline metal atom provides only electrons to the existing band structure. The electrons being introduced during the intercalation process occupy the available electronic states and raise the Fermi level according to the state density function,  $N(E)$ , in the cathode material.

Since in the electrochemical cell of A/liquid electrolyte/ $\text{A}_x\text{MX}_2$ -type the anode potential is constant (concentration of  $A^+$  ions in the electrolyte is constant), it can be assumed that the variations in open-circuit voltage (OCV) of the cell with the concentration of intercalated species are those of the electrochemical potential of electrons (Fermi level) in the cathode material.

High density of states near the Fermi level should lead to a weak dependence of the potential on the concentration of the intercalated species, whereas low density of states should lead to significant variations of the potential with composition. For instance, in the case of titanium and vanadium ( $\text{TiS}_2$ ,  $\text{VS}_2$ ), for which the 3d-band is relatively wide, the high density of states near the Fermi level leads to the classical monotonous character of the dependence of the potential on composition (concentration of intercalated species).

For the oxides of transition metals situated further to the right in the periodic table (Fe, Co, Ni) there is an increasing tendency to form a narrow-band electronic structure. The said tendency may still increase during the intercalation process due

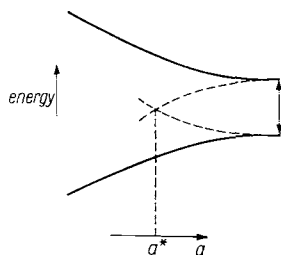


Fig. 1

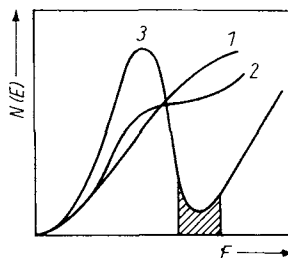


Fig. 2

Fig. 1. Splitting of the effective energy band with increasing interatomic distance [7]. ( $a$  lattice parameter)

Fig. 2. Modified state density function for the cathode material [7]. (1) one-electron approximation (for the starting material), curves (2) and (3) correspond to the increasing interatomic distance, hatched area localized states

to the changes of the interatomic distance. The increase in M-M distance (increase of lattice parameter  $a$ ) decreases the overlap of the  $t_{2g}$ -orbitals spread along the axis joining these atoms in the layer built up of the octahedra and thereby brings about a splitting of the effective energy band. Fig. 1 shows the splitting of the energy band due to the increasing interatomic distance [7]. Shrinkage of the 3d wave functions can lead to a discontinuous density of states  $N(E)$  with energy regions where the charge carriers are localized. Fig. 2 illustrates the modified state density function [7]. Such a modification brings about abrupt changes of the Fermi level and also of the electronic properties of the cathode material. The modification of band structure leading to the splitting of the effective energy band may bring about a change of the nature of the electronic states giving a Mott transition of metal-non-metal type.

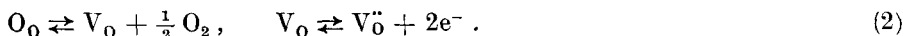
A modification of the electronic structure of the cathode material, taking place during the electrochemical intercalation (formation of a narrow-band structure), should lead to the occurrence of the characteristic plateaux on the discharge curve which is observed for  $Na_xCoO_2$ .

### 3. Results and Discussion

The results presented earlier [4, 5] concerning cobalt bronze  $Na_xCoO_{2-y}$  (P2-structure) have shown that it exhibits a complex structure of ionic and electronic defects. There are deviations from stoichiometry in the sodium and oxide sublattices and both kind of defects introduce electronic carriers. The band structure of cobalt bronze is formed mainly from the 3d-orbitals of cobalt.

For a strictly stoichiometric phase  $NaCoO_2$  the trivalent cobalt ions are in the low-spin state  $t_{2g}^6$ . This state corresponds to a completely filled band. The nonstoichiometry in the sodium sublattice ( $V'_{Na}$ ) accounts for the presence of tetravalent cobalt ions. The low-spin states of the ions,  $Co^{+3}(3d^6)$  and  $Co^{+4}(3d^5)$ , in  $Na_xCoO_{2-y}$  correspond to a partially filled band,  $t_{2g}$  (holes).

The nonstoichiometry in the oxide sublattice introduces donor centres (oxide vacancies,  $V_O$ ) being formed in the following reaction:



The electrons formed as a result of ionization of these centres undergo recombination with holes (related to the nonstoichiometry in the sodium sublattice) lowering their effective concentration, this being described by the equation [4]



The effective charge transport (that of holes) in the cobalt bronze takes place in the  $t_{2g}$ -band, the width of which insures almost metallic properties [4].

From the above discussion it follows that the location of the Fermi level in the cobalt bronze depends on the concentration of electronic carriers related to the nonstoichiometry in the sodium and oxide sublattices. According to the proposed model the variation of the Fermi level with the electronic carrier concentration should manifest itself in the potential of the cathode (e.m.f. of the cell). Fig. 3 (curve 1) illustrates the dependence of the Fermi level changes  $\Delta E_F$  of the starting material  $Na_{0.70}CoO_{2-y}$  on the concentration of electrons introduced chemically into the  $t_{2g}$ -band by varying the nonstoichiometry in the oxide sublattice, (2) and (3).

This relationship has been obtained from the measurements of the starting open-circuit voltage for a series of cells in which the cathode materials had different concentrations of electronic carriers. The material of the highest concentration of holes (lowest  $y$ ) has been selected as a standard for the calculation of the relative changes

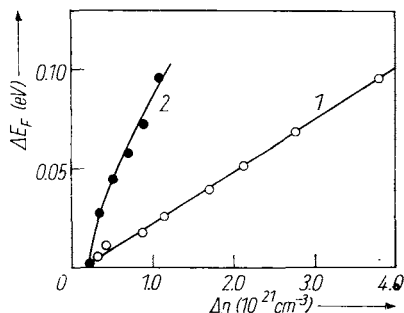


Fig. 3

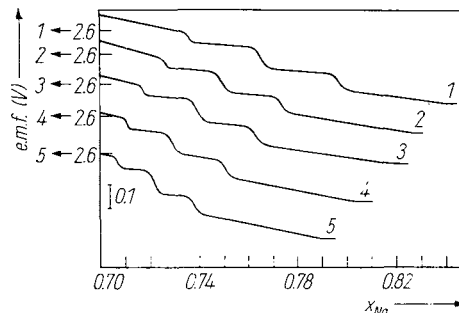


Fig. 4

Fig. 3. Dependence of Fermi level changes  $\Delta E_F$  on electron concentration change in  $\text{Na}_{0.70}\text{CoO}_{2-y}$ . (1) introduced chemically, (2) introduced electrochemically

Fig. 4. Discharge curve (OCV) for  $\text{Na}_{0.70}\text{CoO}_{2-y}$  of different  $y$  (hole concentration): (1)  $y = 0.022$ , (2) 0.033, (3) 0.041, (4) 0.053, (5) 0.073

in the Fermi level. The obtained linear character of the function corresponds to the theoretical model of the Fermi energy variations with the carrier concentration in the transition metal dichalcogenides [8] and is typical of the metallic d-band which is consistent with the almost metallic properties of cobalt bronze.

As already mentioned, during the intercalation the electrons occupy the available electronic states in the electronic structure of the cathode material. Their number depends on the degree to which the starting material is defected. Consequently, the amount of sodium intercalated should depend on the number of states available for electrons. Fig. 4 shows, as an example, a discharge curve for a cobalt bronze  $\text{Na}_{0.70}\text{CoO}_{2-y}$  of different initial concentration of holes.

The concentration of intercalated sodium is equivalent to the concentration of electrons introduced at the Fermi level of the cathode material. It can be noticed that all the curves exhibit two characteristic plateaus occurring at the same potentials, i.e. 2.54 and 2.44 V. The presence of these plateaus cannot be accounted for by any thermodynamic model, since the system is single-phase over the whole range of  $x_{\text{Na}}$  studied [9]. As follows from the figure, the characteristic plateaus are observed at different sodium contents in the same phase. Their location, however, is precisely dependent on the initial concentration of holes. Thus, for instance, the phase of the highest concentration of holes (Fig. 4, curve 1) can incorporate the highest amount of sodium with the equivalent number of electrons on the Fermi level of the cathode material.

It has been stated that chemical introduction of sodium brings about very small changes of lattice parameters in the cobalt bronze (P2-structure) [10]. On the other hand, electrochemical intercalation of sodium results in much bigger changes of the lattice parameters of this material [9]. The observed linear increase of the parameter  $a$  is caused by the increase in the Co-Co distance. According to earlier considerations this change can lead to the modification of the electronic structure in the cobalt bronze.

Fig. 3 (curve 2) illustrates the variations of the Fermi level with the concentration of electrons introduced in the  $t_{2g}$ -band of the cobalt bronze during the electrochemical intercalation process. The Fermi level variations shown in the figure, are those of the open-circuit voltage up to the first potential jump on the discharge curve drawn in Fig. 4. Curve 1 (discussed earlier) refers to the Fermi energy variations with the con-

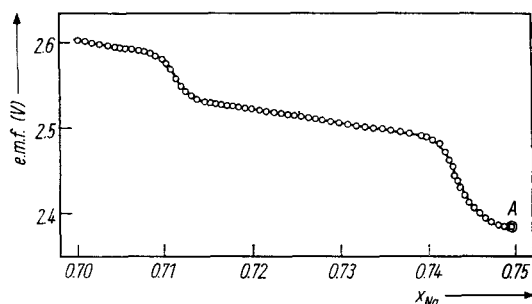


Fig. 5

Fig. 5. Discharge curve (OCV) for  $\text{Na}_{0.70}\text{CoO}_{1.93}$  in the form of a pellet. Point A denotes the composition  $x_{\text{Na}}$  where the work of the cell was broken up

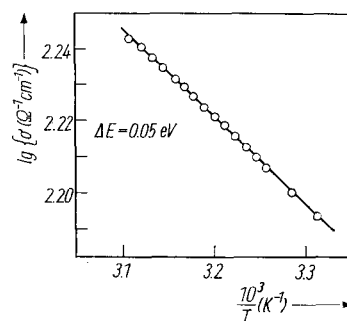


Fig. 6

Fig. 6. Temperature dependence of electrical conductivity for  $\text{Na}_{0.75}\text{CoO}_{1.93}$  (pellet) obtained by electrochemical intercalation from  $x_{\text{Na}} = 0.70$  to  $0.75$

centration of electrons introduced chemically, (2) and (3). Comparison of both curves allows for the statement that significantly less electrons can be introduced electrochemically to the original band  $t_{2g}$ . The original band narrows and becomes filled much faster. The Fermi level rises abruptly and abandons the band (first potential jump on the discharge curve, Fig. 4).

The modification of the electronic structure of the cathode material, taking place during the intercalation process, brings about changes of its properties. The latter have been confirmed in the results of electrical measurements with the cathode material in the form of pellets, after various durations of intercalation.

Fig. 5 presents a discharge curve for the cathode material  $\text{Na}_{0.70}\text{CoO}_{1.93}$  in the form of a pellet. The work of the cathode has been broken up at the moment (point A) when, from the viewpoint of the proposed model, one of the narrow bands produced upon intercalation, has been filled and the filling of the following one has begun.

Fig. 6 presents the temperature dependence of electrical conductivity for a pellet of  $\text{Na}_{0.70}\text{CoO}_{1.93}$ , intercalated up to the composition  $\text{Na}_{0.75}\text{CoO}_{1.93}$  (point A in Fig. 5).

The determined activation energy of conductivity allows for the estimation of the energy gap between the suggested narrow bands, the latter being equal to 0.1 eV and consistent with the abrupt change of the potential on the discharge curve (second potential jump on the discharge curve in Fig. 5, point A). The reversible course of the electrical conductivity variations indicates that its activated character is associated only with an electronic transition and not, for instance, with the rearrangement of the crystal lattice of the bronze. It should be emphasized that for the starting phases studied, i.e.  $\text{Na}_{0.65}\text{CoO}_{2-y}$ ,  $\text{Na}_{0.70}\text{CoO}_{2-y}$ , and  $\text{Na}_{0.75}\text{CoO}_{2-y}$ , for different  $y$ -values the electrical conductivity does not show activated nature over the whole temperature range of cobalt bronze stability, i.e. from 1000 to 4.2 K (electrical conductivity decreases with increasing temperature [4]).

The following example to confirm the qualitative changes in the electronic structure of the cathode material is the difference between the dependences of electrical conductivity and thermoelectric power on the concentration of electrons introduced chemically (by changing the value of  $y$ ) and electrochemically. These dependences are illustrated in Fig. 7 and Fig. 8.

In the case when the electrons are introduced chemically the variations of the electrical conductivity and thermoelectric power reflect the compensation effect [4]. On the other hand, the electrons introduced during the electrochemical intercalation

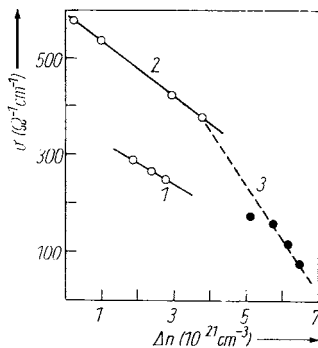


Fig. 7

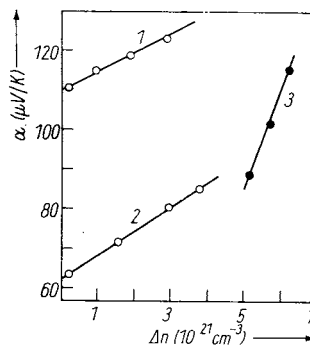


Fig. 8

Fig. 7. Dependence of electrical conductivity of  $\text{Na}_{0.70}\text{CoO}_{2-y}$  on the concentration of electrons introduced (1) under conditions of thermodynamic equilibrium with  $p_{\text{O}_2}$  at 870 K, (2) at 300 K for quenched samples obtained in the temperature range 670 to 970 K and  $p_{\text{O}_2}$  1 to 0.1 atm, (3) under conditions of electrochemical intercalation at 300 K.

Fig. 8. Dependence of thermoelectric power for  $\text{Na}_{0.70}\text{CoO}_{2-y}$  on the concentration of electrons introduced, (1) under conditions of thermodynamic equilibrium with  $p_{\text{O}_2}$  at 870 K, (2) at 300 K for quenched samples obtained in the temperature range 670 to 970 K and  $p_{\text{O}_2}$  1 to 0.1 atm, (3) under conditions of electrochemical intercalation at 300 K.

bring about much stronger changes of these parameters. The stronger decrease of electrical conductivity with the increasing concentration of electrons (introduced during the electrochemical intercalation) is connected with the stronger change of properties of the electronic states (narrowing of the energy bands) rather than with the change of electronic carrier concentration.

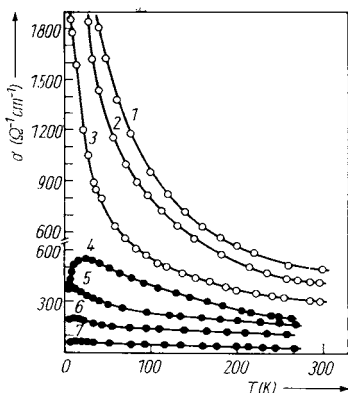


Fig. 9

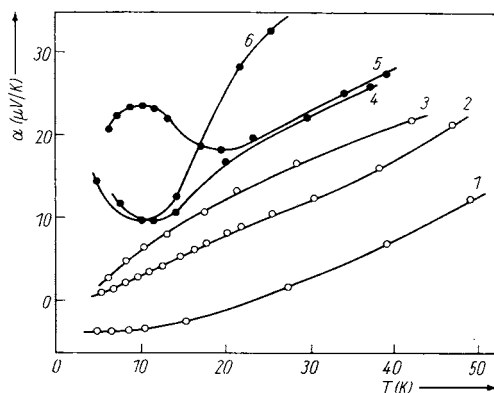


Fig. 10

Fig. 9. Temperature dependence of electrical conductivity of  $\text{Na}_x\text{CoO}_{2-y}$ .  $\circ$  for the starting material ((1)  $\text{Na}_{0.70}\text{CoO}_{2-y}$ , (2)  $\text{Na}_{0.65}\text{CoO}_{2-y}$ , (3)  $\text{Na}_{0.75}\text{CoO}_{2-y}$ ).  $\bullet$  for the intercalated material ((4)  $\text{Na}_{0.75}\text{CoO}_{1.93}$ , (5)  $\text{Na}_{0.77}\text{CoO}_{1.93}$ , (6)  $\text{Na}_{0.79}\text{CoO}_{1.93}$ , (7)  $\text{Na}_{0.80}\text{CoO}_{1.93}$ )

Fig. 10. Temperature dependence of thermoelectric power for  $\text{Na}_x\text{CoO}_{2-y}$ .  $\circ$  for the starting material ((1)  $\text{Na}_{0.65}\text{CoO}_{2-y}$ , (2)  $\text{Na}_{0.70}\text{CoO}_{2-y}$ , (3)  $\text{Na}_{0.75}\text{CoO}_{2-y}$ ),  $\bullet$  for the intercalated material ((4)  $\text{Na}_{0.77}\text{CoO}_{1.93}$ , (5)  $\text{Na}_{0.75}\text{CoO}_{1.93}$ , (6)  $\text{Na}_{0.79}\text{CoO}_{1.93}$ )

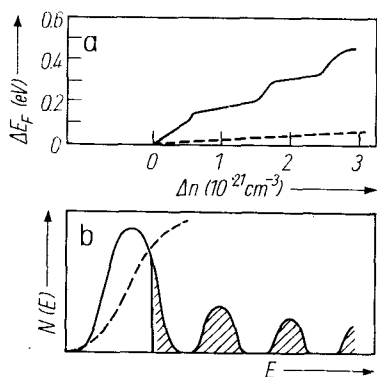


Fig. 11

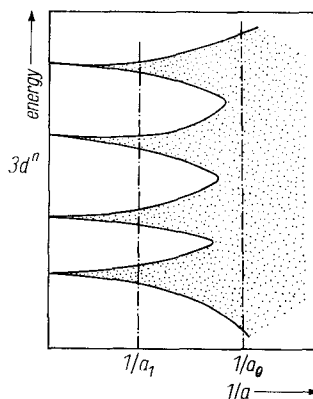


Fig. 12

Fig. 11. Scheme of the electronic model of electrochemical intercalation. a) ——— discharge curve with characteristic plateaus illustrating the variations of the Fermi level as a function of electron concentration introduced in the intercalation process, ---- Fermi level changes as a function of electron concentration in the starting material. b) ——— modification of band structure of the cathode material during electrochemical intercalation, ----  $N(E)$  in one-electron approximation for the starting material, hatched area: localized states

Fig. 12. Scheme of energy bands of cobalt bronze as a function of interatomic separation ( $1/a$ ) for the bands near the Fermi level.  $1/a_0$  denotes the equilibrium location of atoms in the starting bronze,  $1/a_1$  the location of atoms in the intercalated bronze

The change in the nature of electronic states in the cathode material manifests itself in the character of temperature dependences of electrical conductivity and thermoelectric power. Fig. 9 (curves 4 to 7) shows the temperature dependence of electrical conductivity for the intercalated cobalt bronze of various sodium contents obtained by intercalation of the  $\text{Na}_{0.70}\text{CoO}_{1.93}$  phase. In the same figure, for comparison, the characteristics of the starting cobalt bronze are shown (curves 1 to 3). It is clearly seen that the properties of the intercalated bronze differ from those of the starting material. The metallic properties tend to change to the non-metallic ones. The electronic states become more and more localized with increasing amount of intercalated sodium.

Fig. 10 shows the analogous dependences for the thermoelectric power. The values of thermoelectric power for the intercalated phase are higher than those for the starting phase. Moreover, the thermoelectric power for the intercalated bronze (curves 4 to 6) does not come down to zero when  $T \rightarrow 0$ . Such a dependence is typical of the localized states. The qualitative changes of the electronic structure have the nature of the Mott transition of metal-non-metal type, which leads to the formation of very narrow bands in the material.

The results presented here allow for relating the variations of the open-circuit voltage for the electrochemical intercalation reaction directly to the electronic structure of the cathode material. Fig. 11a shows a discharge curve illustrating the variations of the Fermi level of the cathode material as a function of the electron concentration introduced in the intercalation process (solid line). The character of this curve is explained by the modification of the band structure of the cathode material (Fig. 11b — solid line). The electrons being introduced by intercalation fill the original band which, as a result of the suggested modification, narrows and fills up very quickly.

Then filling-up of the next narrow band formed during intercalation takes place. The Fermi level abruptly rises which is manifested by the first potential jump on the discharge curve. On the curve representing the electronic structure of the cathode material this corresponds to the first energy region where the density of states  $N(E)$  is equal to zero. Filling-up of the consecutive bands in the narrow-band structure formed (Fig. 12) manifests itself in stepwise variations of the potential. For comparison, the broken line in Fig. 11b shows the density of states  $N(E)$  for the starting material, described in one-electron approximation. The broken line in Fig. 11a represents the Fermi level  $\Delta E_F$  in this material as a function of the concentration of electrons introduced chemically (Fig. 3, curve 1). If, during the electrochemical intercalation, there were no modification of the electronic structure of the cathode material, the character of the discharge curve would agree with the latter relationship.

### Acknowledgements

The author is grateful to Prof. N. F. Mott for helpful discussion and Prof. P. Hagenmuller, Dr. C. Delmas, A. Stoklosa for discussion and help in carrying out this work.

### References

- [1] A. S. NAGELBERG and W. L. WORRELL, *J. Solid State Chem.* **38**, 321 (1981).
- [2] K. Y. CHEUNG and B. C. H. STEELE, *Proc. Internat. Conf. Fast Ionic Transport in Solids, Electrodes and Electrolytes*, Ed. P. VASHISHTA and J. N. MUNDY, North-Holland Publ. Co. 1979 (p. 141).
- [3] M. S. WHITTINGHAM, *Proc. 5th Australian Electrochemistry Conference*, Ed. D. A. J. RAND, G. P. POWER, and J. M. RITCHIE, Elsevier Publ. Co., Amsterdam-Oxford-New York 1981 (p. 229).
- [4] J. MOLEND, C. DELMAS, P. DORDOR, and A. STOKLOSA, *II. Internat. Conf. Transport in Non-Stoichiometric Compounds, Perpignan-Alenya (France) 1982*, in: *Solid State Ionics*, to be published.
- [5] J. MOLEND, C. DELMAS, and P. HAGENMULLER, *IV. Internat. Conf. Solid State Ionics, Grenoble 1983*, in: *Solid State Ionics*, to be published.
- [6] M. J. SIENKO, *J. Alkali Metals Chem. Soc.* **22**, 429 (1967).
- [7] N. F. MOTT and E. A. DAVIS, *Electronic Process in Non-Crystalline Materials*, Clarendon Press, Oxford 1971.
- [8] J. A. ALONSO and L. A. GIRAFALCO, *J. Phys. Chem. Solids* **39**, 79 (1978).
- [9] J. J. BRACONNIER, C. DELMAS, C. FOUASSIER, and P. HAGENMULLER, *Mater. Res. Bull.* **15**, 1797 (1980).
- [10] J. MOLEND, *Electronic model of intercalation process*, to be published.

(Received September 7, 1983)